

Wide-Angle Coverage Deployable Bunker Antenna for Ground Applications

Sudhakar K. Rao^{id}, *Life Fellow, IEEE*, Maxim Ignatenko, *Senior Member, IEEE*, Suzanna LaMar, Clency Lee-Yow, and Philip Venezia^{id}, *Member, IEEE*

Abstract—Compact and lightweight antennas are required for future ground communication systems to provide wide-angle 4π steradians coverage for man-pack radio communication units carried by soldiers on the ground. Two innovative “Bunker” antennas at K-band are described in this article. The novelty includes antenna deployment from folded to unfolded configurations, compact size, low mass, 4π steradians coverage, low cost, wide bandwidth performance, and built-in radome for protection from severe environmental conditions. Design of these antennas, trades, RF simulations, mechanical design, antenna deployment, and material selection leading to product development are described for the first time in this article. A prototype antenna has been fabricated and measured results are presented. An excellent correlation between measured and simulated patterns has been achieved. The Bunker antenna has very wide frequency bandwidth of 86% covering Ku and Ka secondary frequency bands in addition to its primary K-band and thus could in the future replace three antennas on a dedicated man-pack with a single tri-band antenna solution.

Index Terms—Antenna deployment, bunker antenna, low gain antenna, omni-directional antenna, wide-angle coverage antenna, wide bandwidth antenna.

I. INTRODUCTION

LIGHTWEIGHT and compact millimeter-wave antenna designs enable small unit tactical operations to persist under electronic warfare (EW) conditions. An integrated communications system (ICS) is being developed to protect local, airborne, and reach-back communications from detection, interception and exploitation. The ICS man-pack equipped with advanced antenna technologies, such as the discriminating tri-band Bunker antenna, provides dependable, interoperable, and secure communications both within the unit and with the aircraft the operators are communicating with to exercise a set of highly complex missions. A key mission that will be significantly enhanced with this technology is the close

Manuscript received 5 September 2021; revised 18 March 2022; accepted 2 April 2022. Date of publication 25 April 2022; date of current version 6 October 2022. This work was supported by the United States Air Force and the Defense Advanced Research Projects Agency (DARPA) under Contract FA-8750-18-C-0058. (*Corresponding author: Sudhakar K. Rao.*)

Sudhakar K. Rao is with Northrop Grumman Space Systems, Redondo Beach, CA 90278 USA (e-mail: skraoks@yahoo.com).

Maxim Ignatenko, Clency Lee-Yow, and Philip Venezia are with Custom Microwave, Inc., Longmont, CO 80501 USA.

Suzanna LaMar is with Northrop Grumman Mission Systems, San Diego, CA 92126 USA.

Color versions of one or more figures in this article are available at <https://doi.org/10.1109/TAP.2022.3168723>.

Digital Object Identifier 10.1109/TAP.2022.3168723

0018-926X © 2022 IEEE. Personal use is permitted, but republication/redistribution requires IEEE permission. See <https://www.ieee.org/publications/rights/index.html> for more information.

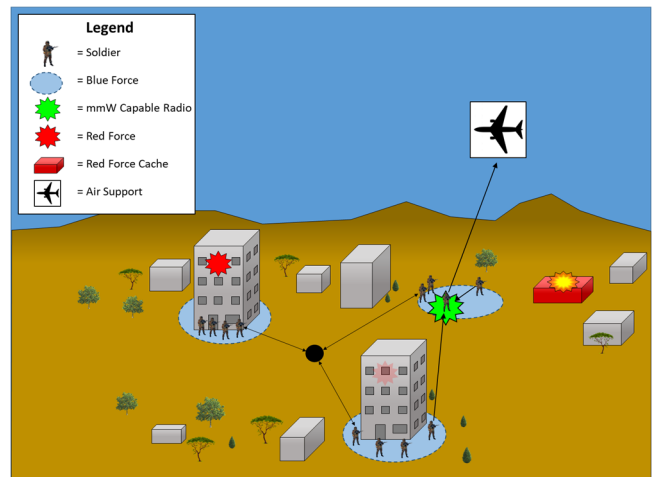


Fig. 1. Millimeter-wave enabling scenario with Bunker antenna.

air support (CAS) mission. CAS is a critical element of joint fire support that employs aircraft fires to destroy, suppress, or neutralize enemy forces to permit movement, maneuver, and control terrain.

Soldiers on the ground require lightweight, enabling technologies, versus currently fielded legacy radios that have many limitations with survivability which will become a liability in the future. The ICS man-pack and the innovative, functional, deployable, and stowable “Bunker” antenna will enable fast, on the move, and at the halt operations to future airborne platforms crucial to both air superiority and establishing air supremacy. Fig. 1 shows a notional scenario using the ICS and the Bunker antenna as part of the soldier’s man-pack unit for communicating with future platforms, to identify, secure, and eliminate the potential adversaries.

Wide-angle coverage antennas with compact size, low mass, and low cost are required for soldiers’ man-pack radio units. In addition, the antennas need to be deployed in two unique configurations: 1) when the soldier is lying down on the ground (communications at the halt “CATH”) and 2) when the soldier is on the move (communications on the move “COTM”). A full coverage of 4π steradians is necessary for these antennas in order to communicate with both aircraft and the ground network infrastructure. This article describes a novel “Bunker” antenna at K-band providing a small, non-invasive, deployable antenna solution in the battlefield that could effectively support communications to ground operators

and/or air vehicles in or near contested environments. The antenna is required for the ICS man-pack applications with deployable configurations. An added capability of the Bunker antenna is that it is designed to support secondary Ku and Ka frequency bands in addition to the primary K-band frequencies where a single tri-band Bunker antenna replaces three separate antennas in the future.

An isotropic antenna with no cross-polarization is used only as a theoretical reference to compare the directional gain of any antenna. In practice, an isotropic coverage over 4π steradians is not realizable as the antenna patterns are affected by the mounting structure, feeding assembly, and scattering effects of the finite antenna structure. A number of low gain wide coverage antennas are described [1], [2] for satellite applications providing either earth coverage of $\pm 9^\circ$ when the satellite is in-orbit or providing a toroidal coverage with peak at 90° with $\pm 20^\circ$ coverage around the peak when the satellite is in the transfer orbit providing telemetry and tracking communications to the ground. The isotropic performance is severely impacted by the mounting structure such as spacecraft and scattering from other support structure and antennas [3]. One way to achieve nearly uniform coverage of a full sphere is to employ a number of switchable quasi-directional antennas pointing in different directions [4]. None of the single antennas cover the entire sphere, but switching them on and off allows a full-coverage pattern to be realized. This approach has drawbacks of increased losses due to switching network, and increased complexity, mass, and cost.

Quasi-isotropic antennas provide uniform power coverage without the control of polarization [5]. Generally, these antennas are made of two orthogonal electric and/or magnetic dipoles. The nulls in the patterns of each dipole are filled by the second dipole with proper amplitude and phase excitation. Examples include two electric dipoles, where proper phasing is achieved by adjusting the length difference of the dipoles [6], four L-shaped monopoles with 90° phase progressions provided by a built-in feed network [7], equivalent electric and magnetic dipoles that are excited in a dielectric resonator antenna [8], U-shape patch [9], and circular sector cavity [10]. In most of the above cases, quasi-isotropic antennas are a quarter wavelength or smaller, and thus they become less than the size of a coaxial connector at frequencies higher than X-band leading to high sensitivity of radiation patterns to mounting platforms, handles, and connectors itself. In this case, having a null in the direction of the platform is beneficial. Unlike quasi-isotropic antennas, omnidirectional antennas with toroidal patterns radiate perpendicularly to their axes with doughnut-shaped patterns having two nulls; one of them can be directed in the direction of the platform. The nulls are typically wide and significantly affect the antenna coverage. A compact antenna using a cavity-backed annular slot operating at L-band is discussed in [11]. This antenna has a narrow bandwidth of 5% and provides less than 2π steradians coverage. A bi-conical antenna (BCA) with narrow elevation coverage is described in [12]. A low-profile dual-polarized wideband omnidirectional antenna was proposed [13] with artificial magnetic conductor (AMC) reflector supporting long term evolution (LTE) band (1.7–2.7 GHz). The antenna structure consists

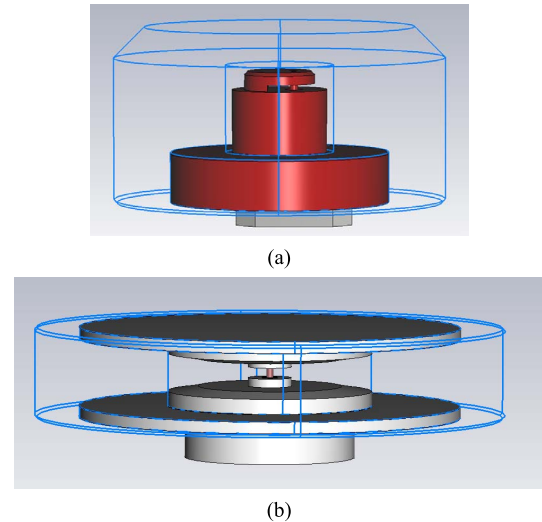


Fig. 2. (a) Bunker inverted-F and (b) Bunker BCAs.

of a horizontally polarized circular loop antenna, a vertically polarized monopole antenna and an AMC reflector. This antenna is too directive with limited coverage. Gronich [14] suggested a small ultra-wideband biconical designed antenna supporting two-octave bandwidths, where an omnidirectional beam in the azimuth plane is achieved, but with limited elevation coverage of only 10° to 20° . Li *et al.* [15] proposed an omnidirectional antenna with wide bandwidth suitable for GSM 1800/3G/LTE/5G indoor communications using printed log-periodical antenna elements, which were evenly distributed around the center to achieve the omnidirectional radiation patterns. Parasitic elements are used here to get the wide bandwidth, but the antenna has drawbacks of larger area, increased complexity and limited coverage. The prior-art literature shows lack of full coverage omnidirectional antennas that are needed for future protected communications used for soldiers' man-pack units.

This article presents two types of antennas as shown in Fig. 2, both capable of providing K-band primary coverage and Ku-band and Ka-band secondary coverages using a single antenna. The first one employs an inverted-F antenna (IFA) providing a cardioid pattern with beam peak perpendicular to antenna aperture resulting in a quasi-isotropic coverage [see Fig. 2(a)]. The second antenna uses an all-metal bi-conical antenna (BCA) with better omnidirectional design and providing a toroidal pattern with beam peak perpendicular to the surface of the antenna [see Fig. 2(b)]. Omni-directional pattern allows for better polarization control, whereas nulls in the patterns are minimized to improve the coverage. By comparing the quasi-isotropic with omnidirectional designs, it is shown that the omnidirectional approach has better coverage for and hence is selected for fabrication and test. This article presents design and performance results of the two Bunker antennas including the unique mechanical configuration for deployment and stowage of these antennas.

Key features of the "Bunker" antenna include: 1) it provides 4π steradians of coverage; 2) the antenna has a novel support mechanism using two fiberglass rods, a conduit, an RF cable inside, clip release mechanism to fold and unfold the antenna

from lying down to standing up positions of the soldier and a 2.92 mm coaxial connector that interfaces with the man-pack radio; 3) it has a protective radome and a small metallic ground-plane; and 4) it is compact and lightweight so that the soldier can carry it easily in the battle-field [16]. Two different antenna types, an IFA and a BCA are initially considered and performance results are presented. Based on the RF performance results, the bi-conical design is selected for prototype fabrication. Measured results of the BCA prototype “Bunker” antenna are presented and compared with full-wave simulations. Additionally, the mechanical deployment of the antenna between the two configurations is demonstrated where the impact of the mechanical support on antenna performance is taken into account.

II. BUNKER ANTENNA REQUIREMENTS

The Bunker antenna carried by the soldier for radio communication with aircraft, headquarters (HQs) and other ground sites within a theater area shall meet the following key primary requirements.

- 1) Frequency range: 20.2 to 21.5 GHz.
- 2) Polarization: RHCP.
- 3) Coverage: 4π steradians.
- 4) Antenna gain: > -6.5 dBic (90% of coverage) and > -9.2 dBic (95% of coverage).
- 5) Return loss: > 10 dB.
- 6) Stowage and deployment: 12” when soldier lying on the ground to 24” when soldier is standing.
- 7) Mass: < 300 grams without support structure and cable.
- 8) Size: 2.5” dia. X 2.0” long (without support rod).
- 9) Protection: Radome cover for field operation.

In addition to the above requirements, the Bunker antenna cost has to be substantially low due to thousands of quantities needed for future man-pack radio applications. The secondary requirements include capability to support Ku-band and Ka-band frequencies in the future where one antenna could replace three different antennas for man-pack radio communications.

III. DESIGN APPROACH

Design optimization and RF analysis of the Bunker antenna are performed using CST Microwave Studio, which is a 3-D full-wave tool capable of efficient modeling of complex EM antenna geometries. The frequency-domain solver used is based on the finite element method (FEM). It automatically refines the mesh in the required areas, thus significantly improving the accuracy with moderate increase in memory and time requirements. The numerical approach is validated by means of measurements.

Antenna patterns were optimized by means of the CST’s covariance matrix adaptation (CMA) Evolution Strategy optimizer. Depending on settings, the optimizer can behave as local or global method. For the Bunker antenna design, the optimizer is set as global. The cost function consisted of an impedance goal and a coverage goal. The coverage goal compares the computed minimal directivity within field-of-view over a given frequency range with the threshold required

directivity value. The reported percentage coverage is relative to full 4π steradians and is evaluated for a given gain value using the following equations:

$$\% \text{ Coverage} = \frac{100}{4\pi} \int_0^{2\pi} d\varphi \int_0^\pi f(\theta, \varphi) \sin\theta d\theta \quad (1)$$

where the function $f(\theta, \varphi)$ is given as

$$f(\theta, \varphi) = \begin{cases} 1, & G(\theta, \varphi) \geq G_{\text{threshold}} \\ 0, & G(\theta, \varphi) < G_{\text{threshold}} \end{cases} \quad (2)$$

$G(\theta, \varphi)$ in (2) is the antenna realized gain in the direction of (θ, φ) and $G_{\text{threshold}}$ is the gain threshold level.

The percentage coverage is evaluated for the required threshold gain values of -6.5 and -9.2 dBic. Taking into account a 1.3 dB cable loss and 0.1 dB loss due to mismatch and material losses, the resulting directivity thresholds are -5.1 dBic for 90% coverage and -7.8 dBic for 95% coverage. To account for the polarization mismatch loss, far-field is evaluated in terms of circularly polarized components, and thresholds are applied directly to RHCP component. Angular resolution of 1° is used in both azimuth and elevation in order to get sufficient samples for % coverage evaluation. This design methodology and analyses resulted in successfully developing Bunker antenna hardware that met all the requirements.

IV. FABRICATION AND RECONFIGURABILITY APPROACH

The reconfigurable mechanical assembly (RMA) is the key component, apart from the antenna, that provides deployment and stowage functions when the soldier is standing and when the soldier is lying on the ground in the battlefield respectively. The RMA is common to both types of antennas and hence it is described upfront. The stowed and deployed configurations of the antenna with RMA are shown in Fig. 3. In the stowed configuration, the antenna is far from the soldier’s head and is close to the waist to minimize the radiation intensity for the safety of the soldier. In the deployed configuration, the antenna is above the head by more than 6” to minimize the radiation intensity. Details of the RMA are shown in Fig. 4.

In addition to meeting functional requirements, the design, choice of material, and manufacturing methods are carefully chosen to maximize use of commercial-off-the-shelf (COTS) items to minimize costs. The following components, as seen in Fig. 4, are readily available as COTS from several suppliers: the 2.9 mm flexible coax cable, the 3/4” diameter fiberglass Support Rods A & B, the 3/8” diameter plastic Flexible Conduit, and the 1” diameter PTFE Sleeve.

The “stops” and “stowing clip” are 3-D printed out of ABS plastic and are glued to their respective “support rods.” The base flange is machined from aluminum and is attached to support rod A using metal pins. The antenna aperture is machined from copper and is fed by a coaxial center conductor that is electrically connected to the copper section by soldering. A machined Rexolite radome is glued to the antenna aperture. The radome/antenna aperture assembly and the “flexible conduit” are attached to support rod B using metal pins. Fig. 5 shows the fabricated parts of the RMA. As can be seen, the Bunker Antenna not only uses several COTS items

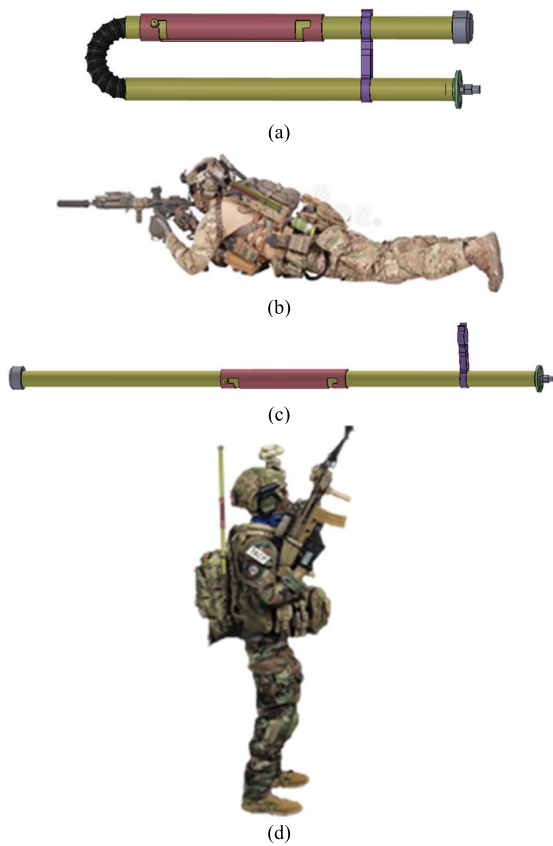


Fig. 3. Antenna integrated with the RMA. (a) Stowed Configuration, (b) soldier carrying K-Band antenna lying down, (c) deployed configuration, and (d) soldier carrying K-band antenna while standing.

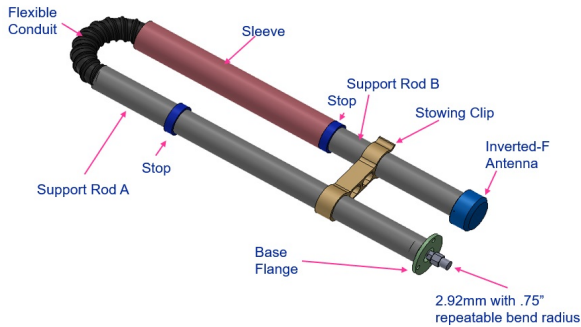


Fig. 4. Details of the RMA showing its parts and construction.

but is also easy to manufacture and assemble. It is lightweight and compact and requires low to no maintenance.

V. INVERTED-F ANTENNA (IFA)

The IFA is optimized for maximizing the antenna coverage in terms of total field and then evaluated with RHCP component of the field. Total field is a combination of co-polarized and cross-polarized field components, and thus the antenna is not designed to distinguish different senses of polarization, but solely to minimize the directivity variation across full sphere. The antenna is expected to behave well in statistical sense in multipath environment when polarization and direction of an incident signal is not known. Antenna's geometry is motivated



Fig. 5. Fabricated RMA prototype showing deployed (top) and stowed (bottom) configurations.

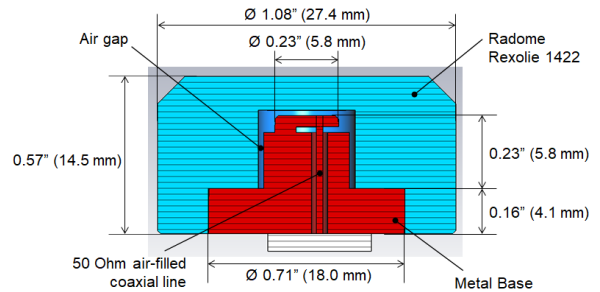


Fig. 6. Inverted-F antenna geometry. A machined radome is glued to the antenna aperture.

by a quasi-isotropic approach based on shorted patch antenna [9], [10]. It also can be regarded as planar Inverted-F antenna. In both cases, the antenna is made of resonant quarter wavelength radiator parallel to ground and shorted on one side. The antenna is fed by a coaxial probe. The offset of the probe from the short determines antenna impedance. At K-band, electrically large ground is needed to accommodate the coaxial connector. Besides, mechanically robust radome is electrically thick. Both ground and radome impact radiation patterns, so that the antenna should be optimized to restore coverage. The proposed IFA consists of two parts, a radiating antenna element and the RMA. The radiating segment comprises an inverted-F antenna fed with a single feed point, a shaped ground plane, a Rexolite radome, and a 2.92 mm coaxial connector. The RMA consists of a coaxial cable, support rods and a conduit for deployment and stowage of the antenna. Fig. 6 shows the geometry of the IFA that includes metallic base, a Rexolite radome with relative permittivity of 2.53 and dissipation factor of 0.00066, an air gap between the top of IFA and the radome for improving the impedance match, a shaped ground plane for widening the coverage and a 2.92 mm coaxial connector interface. The radiating element is moved away from the large base, whereas the thickness of the radome is the result of optimization routine. Details of the RMA are presented in the previous section. The simulated return loss of the IFA including the RMA support structure is plotted in Fig. 7. Return loss is better than 19 dB over the desired band of 20.2 to 21.5 GHz. The 10 dB return loss bandwidth is 35% and is over 16.6 to 23.7 GHz.

Two-dimensional projection of the computed total field directivity along with elevation cuts of the IFA are shown in Fig. 8. They are computed without the mechanical support

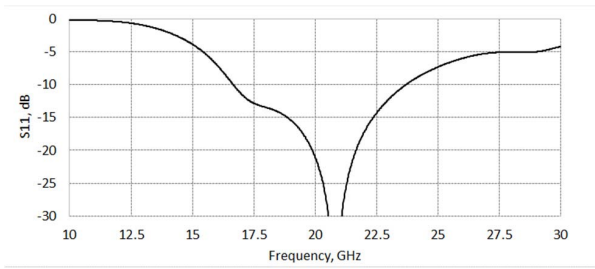


Fig. 7. Computed reflection coefficient of the IFA with frequency. RL is better than 19 dB over 20.2 to 21.2 GHz.

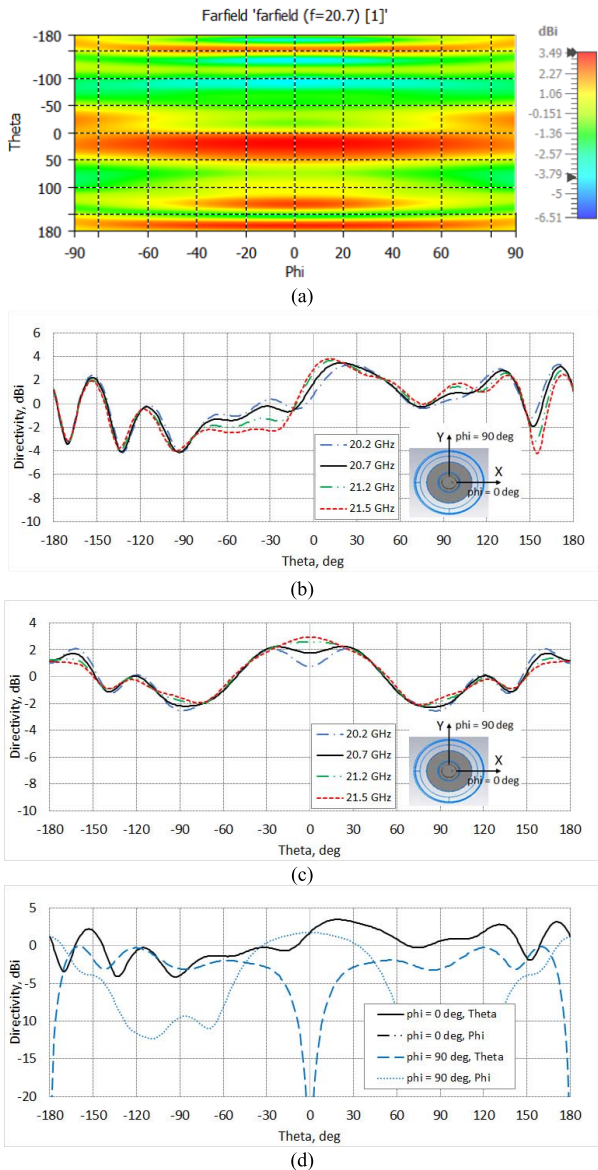


Fig. 8. Computed directivity of total field of quasi-isotropic IFA without support structure RMA. (a) Equirectangular projection at 20.7 GHz, (b) computed elevations cuts in the plane of the pin offset ($\phi = 0$ deg), (c) computed elevation cuts in the plane normal to the pin offset ($\phi = 90^\circ$), and (d) field components in two orthogonal elevation cuts at 20.7 GHz.

structure RMA. The projection at mid-band shows close to quasi-isotropic radiation with directivity variation of 6.3 dBi [see Fig. 8(a)]. Note that the antenna diameter is about 2 wavelengths, which is significantly larger than most of published

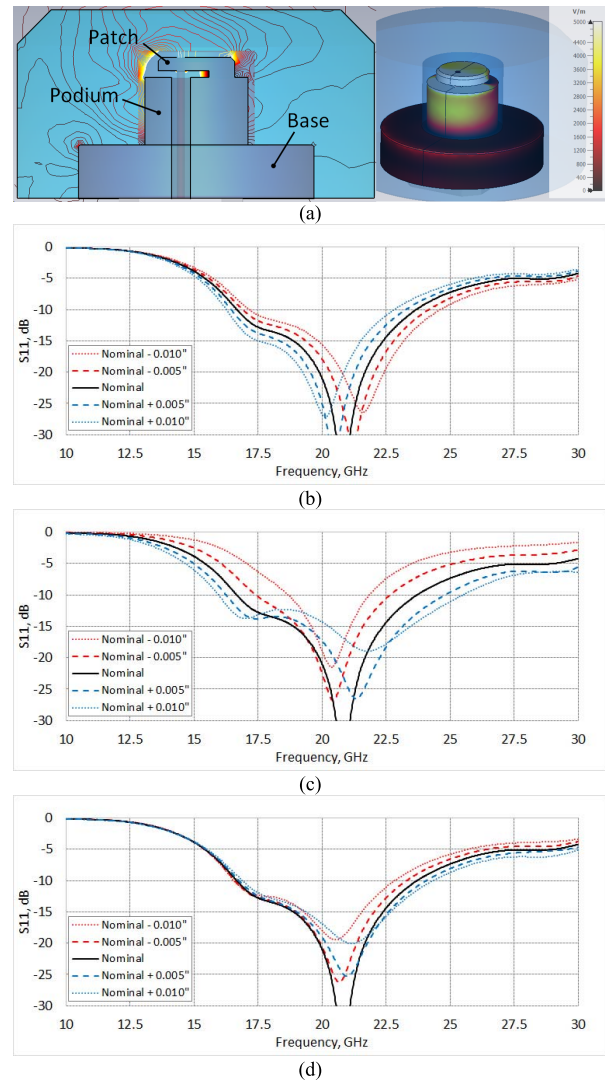


Fig. 9. (a) Distribution of electric field, and sensitivity of reflection coefficient to tolerances of (b) patch diameter, (c) height of the slot between patch and podium, (d) offset of coaxial pin from patch short.

quasi-isotropic antenna designs. Directivity variation can be seen more clearly in elevation θ angle cuts in both XZ and YZ planes [see Figs. 8(b) and (c)]. Polarization of the antenna resembles that of a regular IFA with E-plane in the plane of the feed offset from the short [see Fig. 8(d), $\phi = 0^\circ$]. It is predominantly theta polarized with significant phi component in the vicinity of H-plane.

Distribution of electric field at 20.7 GHz is shown in Fig. 9(a). As expected, the field is maximum next to the feed point, and this is the region determining impedance match. In particular, reflection coefficient is sensitive to the diameter of the resonance patch and thickness of the slot between the patch and podium. Standard dimensional tolerance of CNC machined parts is 0.005" (0.125 mm). Applying this tolerance to the patch diameter or the slot thickness displaces the dip of reflection coefficient, changes its depth, and may even change its shape [see Fig. 9(b) and (c)]. Impedance match is less sensitive to the tolerances of the offset of the coaxial pin from the short [see Fig. 9(d)]. The offset mainly controls the magnitude of the return loss, but whereas its position

TABLE I
VARIATION OF 95% COVERAGE THRESHOLD OF IFA ANTENNA
CAUSED BY FABRICATION TOLERANCES

Variation of Coverage Threshold, dB				
Geometrical Feature		Tolerance	+/- 0.005"	+/- 0.010"
Patch diameter			0.02	0.03
Coaxial pin offset			0.03	0.04
Base diameter			0.09	0.15
Base height			0.07	0.13
Radome diameter			0.04	0.08
Radome height			0.26	0.48
Podium diameter			0.07	0.21
Podium height			0.02	0.18

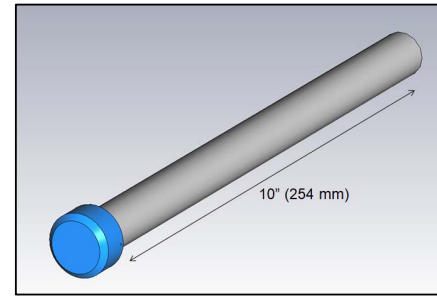
stays the same. Radome is an integral part of the antenna. Without the radome, the return loss is not better than 5 dB from 10 to 30 GHz (not shown). Along with the feed point, electric field is relatively strong at the podium, base, and top of the radome. Sensitivity study shows that reflection coefficient is not sensitive to the tolerances of their dimensions, though they do impact coverage. For the demonstration's sake, the coverage is characterized by the minimal total directivity within 95% of full sphere coverage from 20.2 to 21.5 GHz, which is referred as coverage threshold in Table I. The coverage threshold is most sensitive to the radome height, a bit less sensitive to the dimensions of podium, and even less sensitive to the parameters of base. Clearly, co-designing the well-known radiating element with mounting structure and radome enables wide field of view hardly achievable with original design under given constraints. Overall performance is not sensitive to fabrication tolerances, so it is expected to be consistent for all fabricated units.

The percentage coverages without support structure for two gain threshold values of -7.8 and -5.1 dBic are shown in Table II. As seen, when threshold is applied to total field, the coverage is 100% by design. Coupling to RHCP has lower coverage mainly since IFA radiates both theta and phi far-field components, resulting in high axial ratio at some angles.

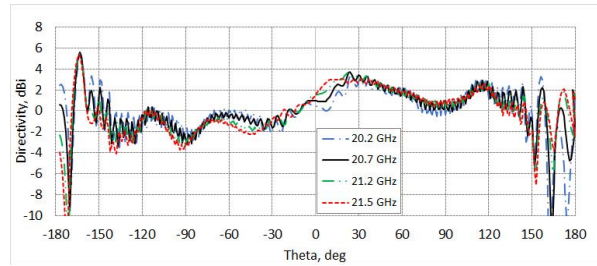
The impact of the support structure RMA on the radiation patterns of the IFA is analyzed using a 10" PTFE rod with cable inside (design of RMA is described later), and it is shown in Fig. 10. The gain variation in the backlobe region is large as could be expected due to the quasi-isotropic shape of the radiation. However, the impact of the support structure on coverage is minimal (see Table II). Even though this antenna has perfect coverage in terms of total field, coverage requirements for RHCP are not fulfilled. An omnidirectional antenna is designed in the next section for better coverage.

VI. BI-CONICAL ANTENNA (BCA)

BCAs are widely used in communication satellites to provide communication links when the satellite is in the transfer



(a)



(b)

Fig. 10. Computed directivity of total field of quasi-isotropic IFA with 10" long support structure RMA. (a) IFA with RMA geometry and (b) computed elevations cuts in the plane of the pin offset ($\phi = 0^\circ$).

TABLE II
CALCULATED MINIMAL PERCENTAGE DIRECTIVITY COVERAGE OF IFA
FROM 20.2 TO 21.5 GHz. THRESHOLD IS EITHER APPLIED TO THE
TOTAL OR RHCP FIELD

Threshold	Total Field		RHCP	
	-7.8dBic	-5.1dBic	-7.8dBic	-5.1dBic
No support structure	100 %	100 %	85.6 %	70.0 %
With support structure	99.7 %	99.4 %	97.8 %	69.8 %

orbit [1] with coverage of $\pm 20^\circ$ around $\theta = 90^\circ$. Transforming dipole arms into cones is a means to improve impedance bandwidth. Radiation pattern is omnidirectional with nulls toward top and bottom of the antenna. Since the antenna is always mounted on a platform, bottom null helps to mitigate the impact of the platform on radiation. Top null impacts the coverage of the antenna and should be minimized.

A few antenna configurations are initially considered, including quadrifilar helix, dipole, bi-conical, and discone antennas. Typical coverage is shown in Table III. Quadrifilar helix antennas are circularly polarized. They can be designed to have wide beamwidth and low axial ratio. Coverage is close to 83% with a small ground plate (ground is 0.16" or 4 mm). However, it significantly drops when connector size is considered (ground is 0.71" or 8 mm). Besides, self-phasing version of the antenna does not have the required bandwidth. Wider bandwidth is achieved with a feed network at the expense of added complexity to the antenna. Omnidirectional antennas are much simpler to design and fabricate. RHCP coverage is from 73% to 86% if connector size is not accounted. This indicates that wide nulls do not prevent from good coverage. When discone antenna is modified to

TABLE III
COVERAGE AT 20.7 GHz OF VARIOUS ANTENNAS

Coverage @ -5.1 dBi Threshold (20.7 GHz)		
Antenna	Total Field	RHCP
Open-Ended Quadrifilar Helix, 0.16" (4 mm) Ground	65.9 %	65.0 %
Printed Self-Phased Quadrifilar Helix, 0.16" (4 mm) Ground	89.3 %	82.8 %
Printed Self-Phased Quadrifilar Helix, 0.71" (18 mm) Ground	64.6 %	54.9 %
Half-Wavelength Dipole	85.3 %	72.5 %
Bi-Conical Antenna	93.6 %	80.9 %
Discone, 0.71" (18 mm) Disc	97.3 %	68.0 %
Discone, 0.36" (9 mm) Disc	93.7 %	85.7 %
Bi-Conical "Bunker" Antenna	99.2 %	92.8 %

accommodate for a connector (0.71" or 8 mm disk), coverage for RHCP drops from 86% to 68%, as expected. Because of the antenna simplicity and encouraging initial results, bi-conical approach is chosen for optimization.

During optimization the following aspects are taken into consideration.

- 1) At K-band, radome provides protection and mechanical support for the top cone as well, so it should have good mechanical strength.
- 2) Flare of the cones can be replaced by steps for easier radome attachment without sacrifice of bandwidth.
- 3) Asymmetric structure helps to manipulate with coverage as it is seen in the results for discone in Table III.
- 4) For this application, the size and mass are reduced by using coaxial feeding (instead of conventional waveguide used for satellites).

The final design extends the coverage over 4π steradians mainly by making cone angle as 0° resulting in reduced radiating aperture size. The BCA provides a dip near the axis perpendicular to the bi-cone aperture over a small region but provides better back lobe performance. Besides, it is mainly theta-polarized, so that polarization loss is 3 dB at all angles. As a result, the percentage coverage is better than that of IFA, and hence is the selected antenna configuration for the man-pack radio. BCA consists of biconical antenna with copper conical structure, airgap, rexolite radome, fiberglass support structure, coaxial cable within the fiberglass rod support and a coaxial connector. The overall size of the antenna without the support structure RMA is 1.9" (48.3 mm) diameter and a length of 0.48" (12.3 mm) (see Fig. 11).

Fig. 12(a) shows distribution of electric field in the antenna. Field is strongest next to the feed point in gap 1, and then it propagates through gap 2 to be radiated from the slot made of top and bottom cones. Sensitivity analysis indicates that reflection coefficient is the most sensitive to the tolerances of the height of gap 1 and gap 2, and diameter of gap 1 [see Fig. 12(c) and (d)]. Tolerances of other geometrical features

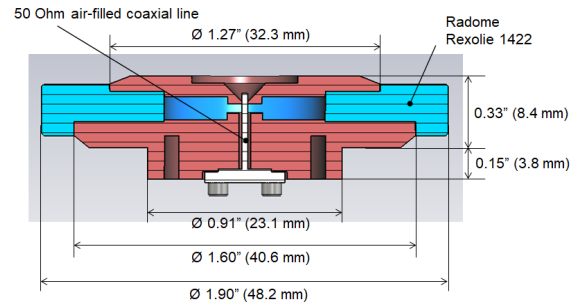


Fig. 11. Geometry of BCA. A machined radome is glued to the antenna aperture.

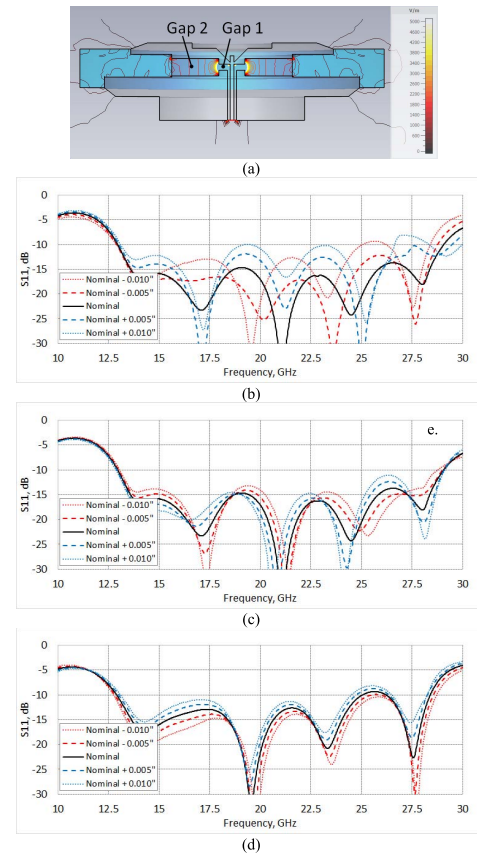


Fig. 12. (a) Distribution of electric field and sensitivity of reflection coefficient to the tolerances of (b) height and (c) diameter of central gap next to the coaxial pin (gap 1), (d) height of the middle gap (gap 2).

do not impact reflection coefficient much. Moreover, even without radome the antenna has impedance match better than 10 dB from 18.5 to 33.5 GHz (not shown). Variation of 95% coverage threshold follows the trend of the reflection coefficient sensitivity (see Table IV). In addition to the heights of gap 1 and gap 2, the coverage is impacted by the diameters of cones and radome. Variation of coverage threshold seems more significant compared to IFA; however, this reflects the fact that the antenna parameters influence the width of null in radiation pattern. Overall design is slightly more sensitive to the fabrication tolerances compared to IFA, with special care to be taken to the height and diameter of gap 1 and height of gap 2.

TABLE IV
VARIATION OF 95% COVERAGE THRESHOLD OF BCA ANTENNA
CAUSED BY FABRICATION TOLERANCES

Variation of Coverage Threshold, dB			
Geometrical Feature	Tolerance	Variation of Coverage Threshold, dB	
		+/- 0.005"	+/- 0.010"
Gap 1 height		0.46	1.13
Gap 1 diameter		0.03	0.03
Gap2 height		0.49	0.58
Gap 2diameter		0.04	0.02
Radome outer radius		0.18	0.36
Top cone diameter		0.22	0.52
Bottom cone diameter		0.15	0.27

TABLE V
CALCULATED MINIMAL PERCENTAGE DIRECTIVITY COVERAGE OF BCA
FROM 20.2 TO 21.5 GHz. THRESHOLD IS EITHER APPLIED TO THE
TOTAL OR RHCP FIELD

Condition	Threshold	Total Field		RHCP	
		-7.8dBi	-5.1dBi	-7.8 dBi	-5.1 dBi
No support structure		99.9 %	99.8 %	99.8 %	92.4 %
With support structure		99.9 %	99.8 %	99.8 %	92.5 %

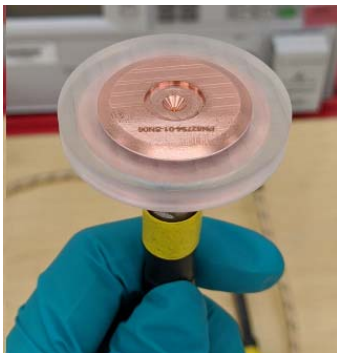


Fig. 13. Prototype unit of the BCA fabricated with a protective radome cover and the RMA.

Calculated percentage coverage for BCA without and with supporting structure are shown in Table V. Relative permittivity of the handle is 5. The antenna satisfies the coverage requirements for RHCP component in both cases.

Six prototype units of the BCA have been fabricated along with their RMAs. The fabricated BCA along with the protective radome and RMA is shown in Fig. 13. The antenna without RMA is very compact and is 1.9" (48.3 mm) diameter and 0.48" (12.3 mm) long with low mass of 66 grams. Measured return loss of the 6 units along with computed results are shown in Fig. 14. Consistency of the measured results among the units indicate that the fabrication tolerances are much better than it was anticipated in Fig. 12. The return loss is better than 19 dB over the desired K-band frequencies.

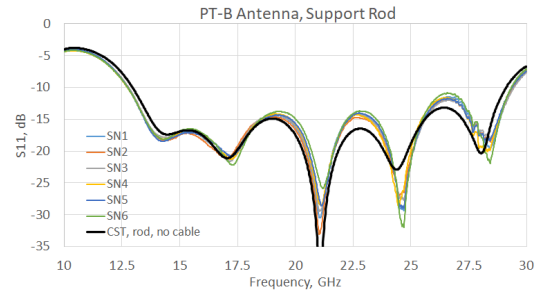


Fig. 14. Measured reflection coefficient of six units of BCA including RMA and comparison with simulated results using CST. BCA exhibits wide bandwidth performance with RL better than 10 dB over 12.5 to 29.0 GHz.

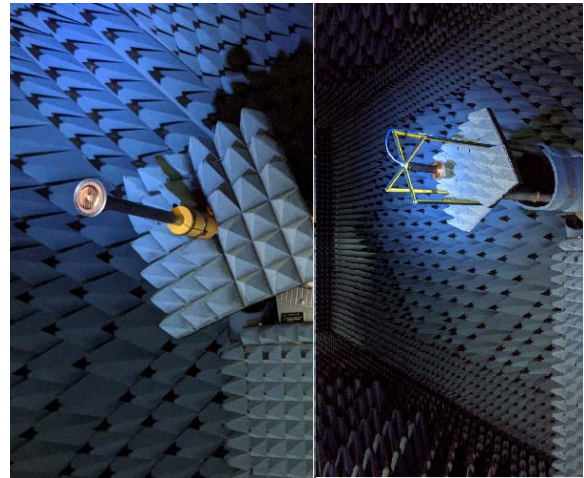


Fig. 15. Anechoic chamber test set-up for radiation pattern measurements of BCA in deployed configuration: (Top Left) Forward Radiation in deployed state. (Top Right) Backward radiation in deployed state.

It shows wide bandwidth of 12.5 to 29 GHz with return loss better than 10 dB over 80% bandwidth. The wideband capability of the BCA allows the unit to support multiple missions at Ku-, K-, and Ka-bands thereby reducing the number of antennas carried by the soldier.

The radiation pattern measurement of the BCA is not an easy task. This is due to the fact that the antenna has low gain, full 4π steradians coverage, and the back lobe pattern measurements need special attention to the support structure. They have been measured in an anechoic chamber and the set-ups used for forward radiation and backward radiation are shown in Fig. 15. It is to be noted that special care has been taken for the backward radiation set-up where non-metallic support structure (made of wood) is used to support the BCA causing reduced scattering effects and an absorber material covering the positioner. Example of measured forward radiation patterns in the forward direction (θ from -90° to $+90^\circ$) is shown in Fig. 16 for the six units along with computed patterns shown in dark red at center frequency. The radiation patterns of the six units track well and match closely with the simulated patterns using CST.

Measured radiation patterns in the backward hemisphere have been measured with the test set-up shown in Fig. 15 where care is taken to support the BCA with non-metallic wooden support structure so that the antenna

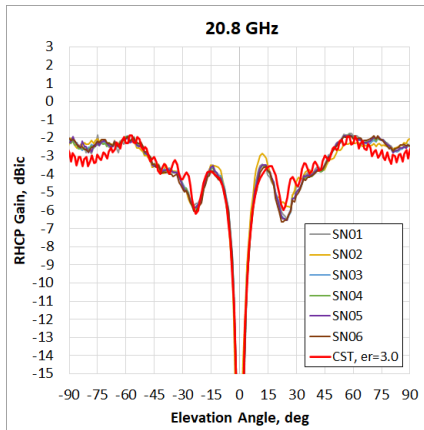


Fig. 16. Measured forward radiation patterns of the six prototype BCA units at 20.8 GHz. Simulated pattern is shown as dark red curve.

TABLE VI

COMPLIANCE OF BCA WITH THE REQUIREMENTS

Requirement	Required	Achieved
Impedance bandwidth, GHz	20.2~21.5	12.7~27.7
Performance bandwidth, GHz	20.2~21.5	20.2~21.5
Polarization	RHCP	Equivalent RHCP (*)
Coverage of 4 π :		
-6.5 dBic	90%	90.6%
-9.2 dBic	95%	97.4%
Weight (no handle, cable), g	300	66
Size, in	2.5" x 2.0"	1.9" x 0.5"
Size, mm	63.5 x 50.0	48.3 x 12.7
Protection	Radome	Radome

(*) Antenna is theta polarized; however, polarization mismatch is accounted in the coverage calculation.

remains stationary while the positioner is moving. Also, absorber material is placed behind the BCA to shield the scattering from the positioner. Radiation pattern at center frequency is shown in Fig. 17 and is compared with simulated pattern. A good agreement is obtained between measurements and simulations. The disagreement is mostly in the areas of deep nulls that got filled due to measurement uncertainties caused by low gain and scattering from the set-up as can be expected.

The measured performance of the BCA is summarized in Table VI and compared with the requirements of the K-band man-pack antenna. The BCA meets all the requirements for each of the six antennas manufactured and the RF performance tracks well among the units in terms of measured return loss, gain, and shape of the radiation patterns. The antennas have wide bandwidth covering K-band primarily as well as secondary Ku- and Ka-bands. This allows a single tri-band BCA replacing three different antennas on the man-pack radio thereby reducing mass, complexity, and cost for future

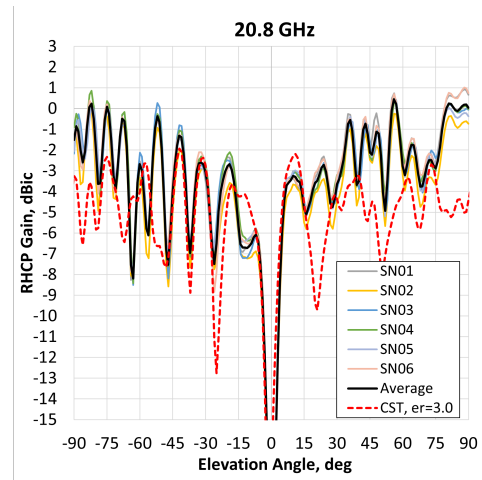


Fig. 17. Measured backward radiation patterns of the six prototype BCA units at 20.8 GHz. Simulated pattern is shown as dark red curve.

protected communication systems. The development of a tri-band antenna is being considered currently. In addition to the man-pack applications on the ground, the BCA and IFA are planned for use in current UAV and aircraft applications.

VII. SUMMARY AND CONCLUSION

This article presents novel antenna designs requiring full 4 π steradians coverage used for soldiers' man-pack units in battle situations for CATH and COTM for future protected communications. Two different antennas, IFA and BCA, are presented where the antennas are compact and deployable from a lying down position to standing position of the soldier without breaking the communication links. BCA has better gain performance over the coverage and measured results match reasonably well with computed results. The antenna is designed with a protective cover and the mechanical deployment mechanism is sealed for debris for field operations. The BCA is capable of supporting K-band primary communications, but also supports secondary communications required at Ku and Ka frequency bands due to its wideband characteristics. In future, the wideband BCA will replace three separate antennas on soldiers' man-pack units with a single antenna resulting in much-needed savings in terms of mass, volume, and cost for protected radio communications.

ACKNOWLEDGMENT

Any opinions, findings, and conclusions or recommendations expressed in this material are those of the author(s) and do not necessarily reflect the views of the United States Air Force and DARPA.

REFERENCES

- [1] S. Rao, F. Mayol, M. Padilla, R. Sudarsanam, and S. Chun, "Array antennas and low-gain TT&C antennas," in *Handbook of Reflector Antennas*, vol. 2. Norwood, MA, USA: Artech House, 2013, ch. 9, pp. 299–349.
- [2] F. Mayol, M. Padilla, and J. M. Montero, "Turnstile-junction-based omnidirectional antennas for space applications [Antenna Applications]," *IEEE Antennas Propag. Mag.*, vol. 53, no. 3, pp. 255–262, Jun. 2011.

- [3] S. Rao, C.-C. Hsu, and R. Sudarsanam, "Low gain antenna performance impact due to spacecraft scattering," in *Proc. IEEE Antennas Propag. Soc. Int. Symp.*, Jul. 2010, pp. 1–4.
- [4] Z. Zhang, X. Gao, W. Chen, Z. Feng, and M. F. Iskander, "Study of conformal switchable antenna system on cylindrical surface for isotropic coverage," *IEEE Trans. Antennas Propag.*, vol. 59, no. 3, pp. 776–783, Mar. 2011.
- [5] W. Scott and K. Hoo, "A theorem on the polarization of null-free antennas," *IEEE Trans. Antennas Propag.*, vol. AP-14, no. 5, pp. 587–590, Sep. 1966.
- [6] G. Pan, Y. Li, Z. Zhang, and Z. Feng, "Isotropic radiation from a compact planar antenna using two crossed dipoles," *IEEE Antennas Wireless Propag. Lett.*, vol. 11, pp. 1338–1341, 2012.
- [7] C. Deng, Y. Li, Z. Zhang, and Z. Feng, "A wideband isotropic radiated planar antenna using sequential rotated L-shaped monopoles," *IEEE Trans. Antennas Propag.*, vol. 62, no. 3, pp. 1461–1464, Mar. 2014.
- [8] Y. M. Pan, K. W. Leung, and K. Lu, "Compact quasi-isotropic dielectric resonator antenna with small ground plane," *IEEE Trans. Antennas Propag.*, vol. 62, no. 2, pp. 577–585, Feb. 2014.
- [9] Y. Pan and S. Zheng, "A compact quasi-isotropic shorted patch antenna," *IEEE Access*, vol. 5, pp. 2771–2778, 2017.
- [10] Q. Li, W.-J. Lu, S.-G. Wang, and L. Zhu, "Planar quasi-isotropic magnetic dipole antenna using fractional-order circular sector cavity resonant mode," *IEEE Access*, vol. 5, pp. 8515–8525, 2017.
- [11] H. Coleman and B. Wright, "A compact flush-mounting antenna with direction finding and steerable cardioid pattern capability," *IEEE Trans. Antennas Propag.*, vol. AP-32, no. 4, pp. 412–414, Apr. 1984.
- [12] C. A. Balanis, *Antenna Theory: Analysis and Design*, 3rd ed. Hoboken, NJ, USA: Wiley, 2005.
- [13] J. Wu, S. Yang, Y. Chen, S. Qu, and Z. Nie, "A low profile dual-polarized wideband omnidirectional antenna based on AMC reflector," *IEEE Trans. Antennas Propag.*, vol. 65, no. 1, pp. 368–374, Jan. 2017.
- [14] I. Gronich, "Omni directional ultra wideband asymmetric biconical antenna," in *Proc. IEEE Int. Conf. Microw., Commun., Antennas Electron. Syst.*, Nov. 2009, pp. 1–4.
- [15] L. Li, W. Yan, B. Feng, and L. Deng, "A wideband omni-directional antenna based on printed log-periodic element," in *Proc. IEEE 3rd Int. Conf. Electron. Inf. Commun. Technol. (ICEICT)*, Nov. 2020, pp. 719–720.
- [16] M. Ignatenko, S. Rao, C. Lee-Yow, P. Venezia, and S. Lamar, "Compact wide angle coverage antenna for air and ground applications," U.S. Patent Appl., Aug. 2021.



Sudhakar K. Rao (Life Fellow, IEEE) received the B.Tech. degree from the National Institute of Technology at Warangal, Warangal, India, in 1974, the M.Tech. degree from IIT Kharagpur, Kharagpur, India, in 1976, and the Ph.D. degree from IIT Madras, Chennai, India, in 1980, all in electrical engineering.

He worked with ECIL, Hyderabad, India, from 1976 to 1977, and LRDE, Bengaluru, India, from 1980 to 1981. From 1981 to 1982, he worked as a Post-Doctoral Fellow with the University of

Trondheim, Trondheim, Norway, and later from 1982 to 1983 at the University of Manitoba, Winnipeg, MB, Canada. He is currently working as an NG Technical Fellow with Northrop Grumman Space Systems, Redondo Beach, CA, USA, providing technical leadership for all divisions of Northrop Grumman in the areas of antennas and payloads for various key programs and proposals. Over the past 40 years, he worked with Spar Aerospace Ltd., Ste-Anne-de-Bellevue, Quebec, Canada, Boeing Satellite Systems, El Segundo, CA, Lockheed Martin Corporation, Newtown, PA, and also with Northrop Grumman and contributed to antennas and payloads for more than 85 different satellite programs and for ground systems. His work on development of radiation templates for complex satellite antenna patterns for interference analysis was adopted and recommended by the International Telecommunication Union (ITU)/CCIR in 1992 as the worldwide standard for satellite manufacturers and operators. He has authored over 220 technical articles and was awarded with 57 patents and six trade secrets. He has authored and co-edited three textbook volumes on "Handbook of Reflector Antennas and Feed Systems" that were published in June 2013 by the Artech House. He delivered invited and keynote talks for more than 50 conferences worldwide.

Dr. Rao is also a fellow of IETE. He is also the Founding Member of the WAMS Series of Symposia in India starting in 2022. Recently, he has served as the IEEE Fellow Committee Member for 2020 and 2021. He is also a

member of the IEEE Fellow Strategic Planning Subcommittee (FSPS) for 2021. He received several awards, including the IEEE Benjamin Franklin Key Award in 2006, the Delaware Valley Engineer of the Year in 2008, the Asian American Engineer of the year award in 2008, the IEEE Judith Resnik Technical Field Award in 2009 for pioneering work in aerospace engineering, the IEEE Region 6 Outstanding Engineer Award for 2017, and the 2017 Northrop Grumman's President Award. He also received the Distinguished Alumni Professional Achievement Award from his alma mater NIT Warangal in 2016, the IETE's Prof. S. N. Mitra Memorial Award in 2016, and the 2020 IETE's Biman Behari Sen Memorial Award. He has served as the Distinguished Lecturer for the IEEE APS and as an AdCom Member for IEEE APS. He was the Founder and the Chair for the IEEE APS "Industry Initiatives Committee" from 2011 to 2015, the IEEE APS Fellow Evaluation Committee Member from 2015 to 2017, the Founder and the Editor of *IEEE Antennas & Propagation Magazine's* "Antenna Applications Corner," and an Associate Editor of the IEEE TRANSACTIONS ON ANTENNAS AND PROPAGATION, and IEEE ANTENNAS AND WIRELESS PROPAGATION LETTERS (AWPL).



Maxim Ignatenko (Senior Member, IEEE) received the Dipl. Eng. degree from Irkutsk State University, Irkutsk, Russia, in 2002, and the Ph.D. degree from Kyushu University, Fukuoka, Japan, in 2005.

He was a Senior Research Associate with the University of Colorado at Boulder, Boulder, CO, USA, from 2013 to 2019. He is currently with Custom Microwave, Inc., Longmont, CO, USA. His research interests include waveguide components, electrically small antennas, antenna-platform interaction, multiphysics analysis, and millimeter-wave Luneberg lens antennas.



Suzanna LaMar received the B.S. degree in electrical engineering from the University of San Diego, San Diego, CA, USA, in 2001, and the M.S. degree in electrical engineering with an emphasis in signal and image processing from the University of California at San Diego (UCSD), San Diego, in 2006.

She is currently the Chief Engineer with the Emerging Capabilities Development (ECD) Division, Advanced Communications and Distributed Systems (ACDS) Operational Unit (OU), Northrop Grumman Mission Systems, San Diego, CA, USA.

Ms. LaMar is also a Northrop Grumman Technical Fellow.



Clency Lee-Yow received the B.Sc. and Ph.D. degrees in electrical engineering from Queen Mary College, London, U.K., in 1983 and in 1987.

He spent one year with the university as a Research Assistant before joining Com Dev International in Cambridge, ON, Canada, where he worked as a Senior Engineer designing a variety of reflector antenna feeds for satellite communications. In 1994, he joined Custom Microwave, Inc. (CMI) and took over as the Vice President of operations. He became the President and CEO of CMI in 1999 and has since

then transformed the company into a major supplier of high-performance reflector antenna feeds for satellite communications. Since that time, CMI has supplied feeds for more than 250 satellite programs.



Philip Venezia (Member, IEEE) studied electrical engineering at the University of Colorado at Boulder, Boulder, CO, USA, from 1998 to 2002. He received the B.S. degree (Hons.) in electrical engineering from the University of Colorado at Boulder, in 2002.

He has been working with Custom Microwave, Inc., Longmont, CO, USA, since 2004, where he is currently the Director of engineering. He has published several papers in technical conferences and journals and has ten U.S. patents. His current research interests include reflector antennas, multi-frequency antenna feeds, and extremely high-performance passive waveguide components for use in the space industry.